Electrospray Mass Spectrometry for In-Orbit Biomolecule Analysis

Shawn P. Cogan
Institute of Space Systems
Stuttgart University
Stuttgart, Germany
st149655@stud.uni-stuttgart.de

Zach Ulibarri
Sibley School of Mechanical and Aerospace Engineering
Cornell University
Ithaca, New York, USA
zulibarri@cornell.edu

Elaine Petro
Sibley School of Mechanical and Aerospace Engineering
Cornell University
Ithaca, New York, USA
epetro@cornell.edu

Amy E. Hofmann
Jet Propulsion Laboratory
California Institute of Technology
Pasadena, California, USA
amy.e.hofmann@jpl.nasa.gov

***Abstract*—Here we describe a suite of experiments probing the ability of ESI propulsion sources to serve as TOF-MS ionization stages in pure vacuum operation. The goals of the study are to assess the operational parameter space which may result in biomolecules entrained in an ion spray, detectable by traditional mass spectrometry techniques. The variables explored in this work include the ionic liquid solvents EMI-BF_4 and EMI-Am, and biomolecules arginine and cellulose. A laboratory ESI source is coupled with a TOF-MS capable of providing a mass resolution (m/dm) between 200 and 1000 for the ion range of interest (100-500 amu). The ion spray is characterized with the solvent alone and with the biomolecules mixed in. Initial experiments indicate that cellulose may be detectable at high concentrations in EMI-BF_4 while operation with EMI-Am may require heating above room temperature.**

1. Nomenclature

d	$[m]$	Distance between emitter tip and extractor plate
e	$[C]$	Elementary charge
E	$[V/m]$	Electric field strength
ΔG	$[eV]$	Solvation energy
I	$[A]$	Emitted current
m	$[u]$	Atomic mass unit
m_i	$[kg]$	Mass
q	$[C]$	Electric charge
t	$[s]$	Flight time
v	$[m/s]$	Particle velocity
V_{start}	$[V]$	Startup voltage required to form a Taylor cone
z	$[-]$	Number of elementary charge units

Greek Symbols

ε	$[-]$	Relative permittivity
ε_0	$[\frac{s^4A^2}{m^3kg}]$	Permittivity of free space
Θ	$[^\circ]$	Half angle of portion of plume impacting detector
Φ	$[V]$	Electric potential
Φ_0	$[V]$	Emitter tip electric potential
Φ_g	$[V]$	Gate electrodes electric potential

978-1-6654-9032-0/23/$31.00 ©2023 IEEE

2. Introduction

Mass spectrometers are a common type of instrument used to study the chemical composition of samples, with applications ranging from pharmaceuticals and forensics to biology and space exploration [1]. Time of flight mass spectrometry (TOF-MS) systems aboard spacecraft have been used to study the composition of space-borne dust grains ejected from icy ocean worlds, such as Enceladus [2]. Because icy ocean worlds are known or suspected to harbor liquid water oceans underneath their crusts of surface ice, they are often considered prime candidates for habitability assessments and biosignature searches [3]. Such missions would seek to study the inventory of complex organics at these icy moons and determine if any complex organics or biomolecules are present, e.g. [4]. However, TOF-MS analysis requires that the molecules of the sample be ionized so that they can be accelerated via an electric field towards a detector. The ionization process itself may fragment larger, complex organic molecules. Therefore just before the sample's molecules are characterized, they may be altered by the ionization process, leading to incorrect identification of the sample composition. Terrestrially, electrospray ionization (ESI) is employed in many TOF-MS systems because it minimizes fragmentation of biomolecules relative to other methods.

In ESI, the sample is ionized as a result of a strong electric field produced by the difference in potentials between an emitter tip and an extractor plate. The liquid sample is drawn to the emitter tip either by external wetting of the needle, or by capillary action through a porous or hollow needle. The emitter is made to be extremely sharp to increase the electric field strength at the tip and to aid in the formation of a Taylor cone, a cone of solution that forms at the needle tip and facilitates ionization. The resulting instability creates charged droplets and ionized molecules, which are accelerated along the potential gradient. When coupled with a TOF system, a long flight path between the ion source and the detectors allows particles to separate based on the inverse-square relationship between their mass and their flight velocity. The differences in flight time are used to calculate mass-to-charge ratios of the ionized particles, from which the chemical composition of the sample can be inferred.

While electrospray ionization mass spectrometry (ESI-MS) has been widely implemented to detect organic samples in terrestrial, clinical settings, it has not been utilized in space exploration for in-situ measurements [5]. While soft ioniza-

2023 IEEE Aerospace Conference | 978-1-6654-9032-0/23/$31.00 ©2023 IEEE | DOI: 10.1109/AERO55745.2023.10115822

tion techniques, and specifically ESI-MS, could be valuable tools for the detection and characterization of complex organic material found throughout the solar system, traditional methods of ESI-MS require modification for use in space; the ionization process must be performed in a vacuum and ideally without a buffer gas, which is typically employed terrestrially. However, ESI sources are routinely used as high specific impulse thrusters for cubesats [6], [7]. These sources are designed to operate natively in space and use specialized ionic liquids that do not evaporate in vacuum. The goal of the present work is to adapt these ESI propulsion devices for use as the ionization stage in spacecraft-mounted mass spectrometers for future missions.

3. Experimental Methods

For this study, arginine and cellulose are chosen as organic molecules that would be prone to fragmentation in traditional mass spectrometer hard ionization methods. They are also molecules critical to life on Earth, and may be similar in structure to organic compounds found in space. Arginine, an amino acid, is necessary for the formation of proteins, similar to another amino acid glycine, of which traces were found in interstellar space [8] and on comet 67P/Churyumov-Gerasimenko and a variety of other abiotic souces [9], [10]. Ionic liquids EMI-BF_4 and EMI-Amino acetate (EMI-Am) are used as solvents to help transport and ionize the organic molecules. EMI-BF_4 is chosen due to its extensive use in vacuum electrospray sources [11], [12]. EMI-Am is chosen because it is commonly used in ESI propulsion and is known to dissolve cellulose [13]. In these experiments, the ESI source is fired at positive voltage, accelerating singly charged EMI^+ molecules and other molecules attached to EMI^+. The mass spectrum of EMI-BF_4 ESI sources has been well characterized [12], and is mostly limited to monomers EMI^+, dimers EMI^+(EMI-BF_4) and trimers EMI^+(EMI-BF_4)$_2$. This is important because precise interpretation of the resulting mass spectra will require the identification of mass lines of both the solvent EMI-BF_4 and any additional lines present when new organic analytes are added.

ESI Source

The ionization source consists of a needle emitter electrode, a liquid reservoir, and an extractor plate. Surface tension and capillary forces draw the liquid sample from the reservoir to the emitter tip. A positive potential is applied to the needle, while the extractor plate is held at ground, as shown in Fig. 1. The needle tip radius is approximately 13 μm and the distance between the needle tip and extractor plate is approximately 1 mm. An example scanning-electron microscope image of a needle is shown in the supplemental Fig. 10. The startup voltage to fire EMI-BF_4 can be estimated from the geometry and liquid with the following relationship:

$$V_{start} = \sqrt{\frac{\gamma r}{\varepsilon_0}} ln\left(\frac{4d}{r}\right) = 1695\ V, \tag{1}$$

where γ is the surface tension of the solvent. The critical electric field at the tip of the Taylor cone is calculated by balancing the energy barrier ΔG of the liquid and the Schottky depression [14]:

$$\Delta G = \sqrt{\frac{e^3 E^*}{4\pi\varepsilon_0}} \Rightarrow E^* = \frac{4\pi\varepsilon_0 \Delta G^2}{e^3}. \tag{2}$$

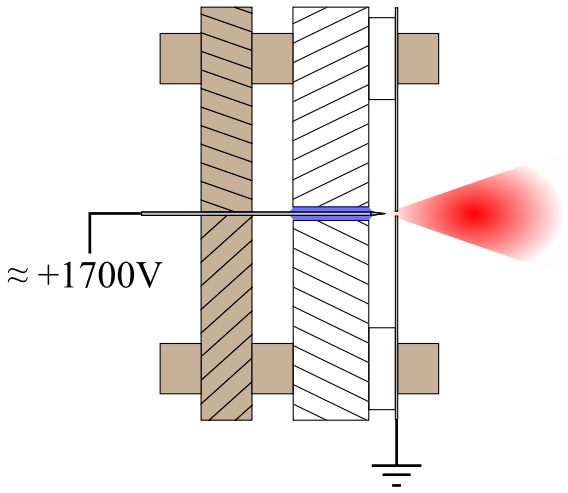

Figure 1. ESI source comprised of an emitter needle, a propellant reservoir and an extractor plate. The beige material is non-conducting polyetherketone (PEEK) plastic, while the white material is aluminum. The blue shaded region near the needle tip is the reservoir, in which ionic liquid was placed.

Table 1. Properties of the ionic liquid EMI-BF_4.

EMI-BF_4	
Permittivity ε	10 [-]
Conductivity K	1.3 [Si/m]
Surface Tension γ	0.052 [N/m]
Solvation Energy ΔG	1.5 [eV]

Given the solvation energy ΔG, the resulting critical electric field necessary for ionization is 1.56 V/nm. The current density is approximated from the permittivity and conductivity values of EMI-BF_4, listed in Table 1 [12]. Thus the predicted emission current from the ESI source is given by:

$$I \approx \frac{32\pi K\gamma^2}{\varepsilon_0^2 E^{*3}} \frac{\varepsilon}{(\varepsilon-1)^2} = 146\ nA. \tag{3}$$

Consistent with these estimates, the ESI source begins firing consistently between 1500 and 2000 V, and emits a current between 100 and 200 nA. Note that steady emission (constant current for minutes or hours of operation) is typically achieved at hundreds of volts beyond that required for startup.

Two emitter types were explored: externally-wetted tungsten needles and porous ceramic emitter tips. The tungsten needles were fabricated from an electrochemically sharpened and etched rod [15]. The ceramic emitter tips were cast from alumina. Both had similar tip radii, which is a critical geometric feature for achieving the desired emission characteristics. In the porous needles, the sample is pulled to the tip through capillary action, while the externally-wetted needle must be coated with the liquid as shown in Fig. 2. No significant differences in emission were observed between emitter types, and the experiments presented within the scope of this paper were carried out using an externally-wetted needle.

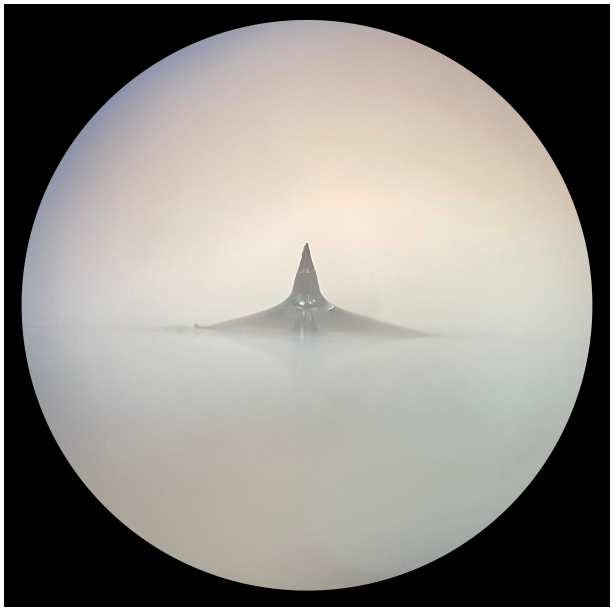

Figure 2. Meniscus of EMI-BF_4 surrounding a tungsten emitter needle.

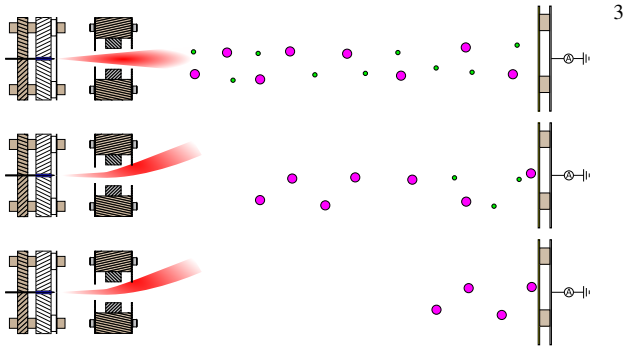

Figure 3. Heavy (purple) and light (green) ion distribution in a TOF system, from top to bottom: at time t_0 just before gate activation, at time t_1 after gate activation, and at time $t_2 > t_1 > t_0$ after gate activation.

TOF System

The vacuum chamber housing the ESI source is fitted with a flight tube, which is a hollow tube that the ions are accelerated down. A detector placed at the end of the flight tube measures the change in current with arrival of different charge-to-mass ratio ions. For these experiments, the ESI source was between 0.5 and 1 meter from the detector, and a vacuum pressure of 10^{-5} Torr was maintained. An electrostatic deflector (described in more detail below) is placed downstream of the ESI source, allowing charged particles to pass at regular intervals, at a frequency of 10 kHz. As outlined in Fig. 3, each pulse of the deflector redirects ions away from the detector and allows evenly mixed particles to separate based on different velocities and masses. The collected current at the detector drops off in discrete steps, indicating the abundance and mass-to-charge ratios of the subspecies in the sample. Once all species have impacted the detector, the deflector is turned off and one cycle is complete. The final result is obtained by averaging over hundreds or thousands of cycles.

Because this project focuses on the ionization source rather than the actual TOF system, the studies shown here have used a minimally complex linear TOF. Higher mass resolutions and increased performance can be attained with a more complex system, such as a reflectron TOF. These enhanced capabilities are not required for the present studies, but they will be beneficial to future investigations of organic mixtures, very high mass organics, and biomolecules.

Electrostatic Deflector—The electrostatic deflector consists of two electrodes with an electric potential between them that is strong enough to completely deflect crossing particles. For the detector aperture of 42 mm and a minimum flight distance of 500 mm, the minimum deflection angle to avoid particle detection is Θ_{min} = 2.4°. The electrodes are held at ±950 V, $d = \frac{1}{2}$ inch apart, and have a width of $\ell = \frac{3}{8}$ inches. At a typical acceleration potential of $\Phi_0 = 3000$ V, the particle deflection is given by:

$$\Theta = tan^{-1}\left(\frac{\Phi_g \ell}{2d\Phi_0}\right) = 13.36°, \tag{4}$$

ensuring particles do not reach the detector while the deflector is active. The deflector electrodes are electrically shielded in the direction of the beam path to avoid unwanted interference.

Mass Resolution—The mass resolution of a mass spectrometer is a measure of how well the instrument can distinguish between adjacent mass lines. It is typically defined as

$$\frac{m}{\Delta m} = \frac{t}{2\Delta t}, \tag{5}$$

where Δm is the difference in mass between adjacent mass lines and Δt is the time width of an ion packet, typically measured as the full-width-at-half-maximum (FWHM). Using conservation of energy, $\frac{1}{2}mv^2 = qV$ (where q is the ion charge, m is its mass, v is its velocity, and V is the accelerating potential) and solving for velocity, the time an ion of mass m takes to reach the detector is calculated as

$$t = L\sqrt{\frac{m}{2qV}}. \tag{6}$$

Substituting into Eqn. 5, the mass resolution can be estimated using the equation

$$\frac{t}{2\Delta t} = \frac{L}{\Delta t}\sqrt{\frac{m}{8qV}}. \tag{7}$$

Assuming an ion packet spread of $\Delta t \approx 20$ ns and an acceleration potential of 2 kV, a mass resolution of $\frac{m}{\Delta m}$ of 200 is achieved for all masses above 100 AMU for a for a flight distance of 0.5 m, and all masses above 22 AMU for a flight distance of 1 m. The high mass range resolution for various flight distances is shown in Fig. 4.

EMI-BF_4 and EMI-Am, as well as the organic molecules being detected, have mass ranges m/z ≈ 150–200, within the margins of temporal resolution of the mass spectrometer. Placing the ESI farther or closer to the detector allows a trade-off between resolving power and signal strength.

Detection— A Hamamatsu F1217-011 microchannel plate (MCP) is used as an electron multiplier and detector, and

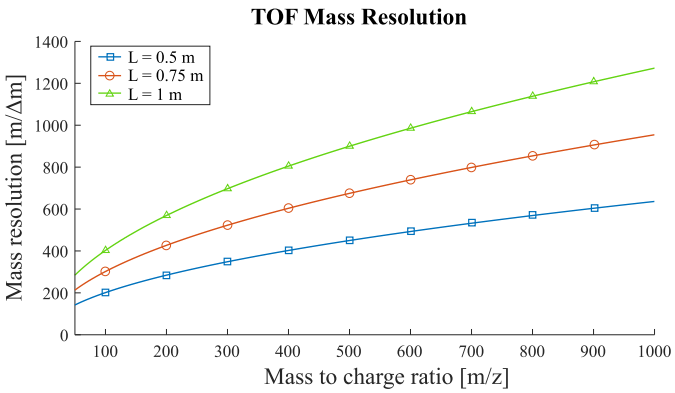

Figure 4. Mass resolution over m/z, assuming Δt=20 ns and Φ_0=2000 V.

it is coupled with a FEMTO fast transimpedance amplifier (TIA). Although the microchannel plate offers a relatively large collection area, there is still a significant loss of current between the ESI and detector, due to beam spreading over the length of the flight tube. Assuming an equal distribution of emission over the surface of a spherical cap with a half angle of ϕ, the portion of the current reaching the detector is equal to

$$I_{detector} = \left(\frac{1 - cos\,(\Phi)}{1 - cos\,(\phi)}\right) I_{emitted}, \tag{8}$$

where $\Phi = tan^{-1}\left(\frac{d}{2L}\right)$ is the half angle of the portion of the plume impacting the detector. Experiments with similar conditions have determined that the half angle of the emitted ion plume is approximately $\phi = 20°$ [16]. At a flight distance of L = 1 m, and an impact diameter of 42 mm, the signal can be reduced by a factor of up to 274. The F1217-011 MCP has a maximum gain of 27.5×10^3, and is coupled with a TIA with a gain of 1×10^4 V/A. The MCP supply voltage regulates the signal gain, and is set to supply a voltage reading of $\approx$ 100 mV from the TIA. Fig. 5 shows the MCP assembly, including grounding wires (white), a supply voltage line (coaxial), and a current signal wire (green).

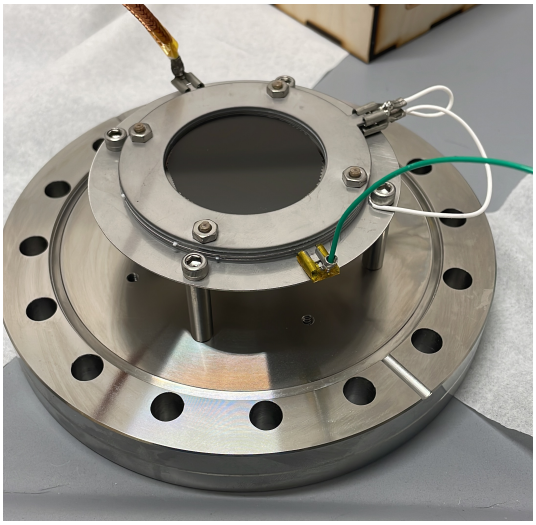

Figure 5. MCP mounting and electrical assembly.

4. Results

As a control, EMI-BF_4 was fired without the addition of organic molecules. The TOF signal was differentiated numerically and the flight time transformed to a m/z ratio using Equation 6. EMI^+ molecules as well as dimers and trimers of EMI-BF_4, were detected in the resulting mass spectrum shown in Fig. 6. This particular spectrum data was collected using a flight distance of 0.621 m and a firing voltage of 3060 V.

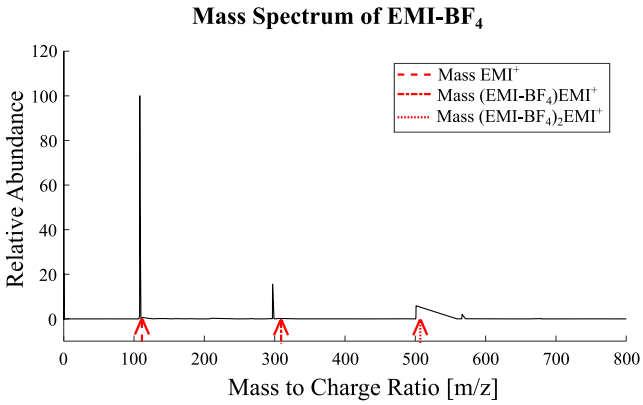

Figure 6. Gathered mass spectrum of EMI-BF_4

Attempts to fire EMI-Am were unsuccessful due to an increase in its viscosity when exposed to vacuum. Its high viscosity readily trapped miniature air bubbles inside the fluid, which expanded during depressurization. The resulting volatile behaviour disrupted the meniscus critical to successful ion emission. Future work will explore increasing the solvent temperature in order to lower its viscosity and improve outcomes. While not the subject of this study, histidine monohydrochloride has been observed to successfully dissolve in EMI-Am, motivating further exploration of its use in future studies.

Noise Reduction

A series of smoothing functions and corrections were applied to the mass spectrum data, to reduce oscillations coupled with gate activation and background noise. The initial oscillations (0-3 μs) may have been due to an impedance mismatch, and are still being investigated. However the timescales of the transients are outside of the range of expected ion flight times. Random noise and MCP dark current was accounted for by subtracting an empty MCP signal (that is, the signal gathered while the ESI source was off). A moving average filter and modified Savitky-Golay smoothing function was applied to remove random peaks, while preserving large drops in current indicative of species detection. The result of each post-processing step is shown in the supplemental Fig. 9.

EMI-BF_4 and Cellulose

Cellulose granules were combined with EMI-BF_4 with a weight ratio percentage of 33%. The mixture was shaken and emulsified to homogenize the mixture, however, separation of undissolved cellulose granules occurred within several hours if the mixture was not directly fired. An agitated sample of the mixture was used to coat the ESI emitter tip, and the resulting TOF signal was recorded (Fig. 7). Overlayed in the figure are arrows indicating the expected flight times of EMI-BF_4 fragmentation species, as well as that of an EMI-BF_4 pair coupled with a cellulose fragment (a single

glucose chain). The observed change in current at 18.45 μs

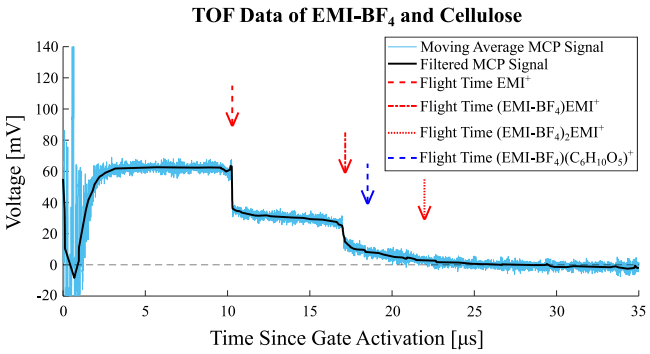

Figure 7. TOF signal of EMI-BF_4 and cellulose with Φ_0=2100 V and flight distance d = 0.621 m.

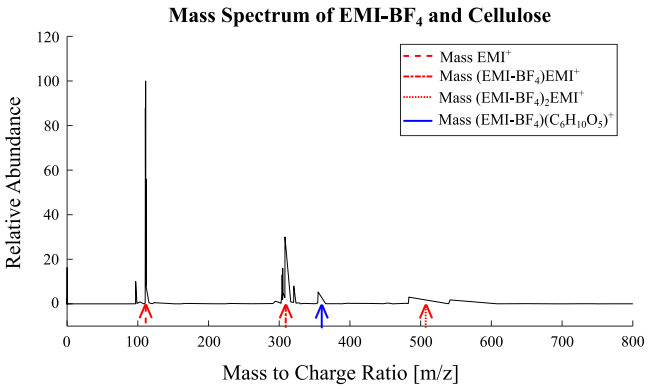

Figure 8. Mass spectrum of a cellulose and EMI-BF_4 mixture.

corresponds to a mass-to-charge ratio of $m/z = 357.7$, which cannot be formed by an integer combination of EMI and BF_4 molecules. However, the mass does correspond to the mass of $C_6H_{10}O_5$(EMI-BF_4) ($m/z = 360$), which is marked with a blue arrow in Fig. 7. It is also noted that this peak is absent from the pure EMI-BF4 mass spectrum (Fig. 6).

A steady decrease in current, visible between 10 μs – 17 μs, is most likely due to fragmentation of dimers, wherein separation of EMI^+ and neutral EMI-BF_4 molecules while the beam is still being accelerated to its final energy causes a steady flux of ions rather than a step change. Separation may occur anywhere in the acceleration stage, leading to the observed distribution of flight times. Similarly, the steady decrease in current beyond 17 μs is most likely due to fragmentation between EMI^+ and larger numbers of EMI-BF_4 molecules, i.e. trimers and higher order species. The resulting mass spectrum (Fig. 8) reflects the possible measurement of cellulose with a relative abundance of 5.3%. EMI-BF_4 does not carry a charge, indicating that the glucose fragment may carry a positive charge and impact the detector while attached to a neutral molecule of the solvent. Alternatively, the peak may be a measurement of (EMI-BF_4)($C_6H_{10}O_5$)EMI^+ molecules that lost the EMI^+ ion after acceleration. In this case, an additional peak at 471 amu of the unfractured ion group is expected, which may not have been accurately resolved due to trimer fragmentation and low resolving power at high mass-to-charge ratios. On the other hand, if such an ion is metastable with a lifetime shorter than the flight time of the system, non-detection of the unfragmented mass may be expected.

EMI-BF_4 and Arginine

In experiments involving a 3:1 mass ratio mixture of EMI-BF_4 and arginine, the organic compound was not detected among the subspecies of the solvent. These results indicate an absence of bonds between the organic molecule and EMI^+, which are necessary for detection. Future work may focus on detection in negative firing mode, and the use of different, more reactive, solvents.

5. Conclusions

These preliminary results of an in-vacuo ESI TOF-MS system show potential feasibility for the gentle ionization of complex organics in future space-borne instruments. Mass spectra of the ionic liquid EMI-BF_4 were taken and mass lines were observed at the expected locations of EMI^+, (EMI$-BF_4$)EMI^+, and (EMI$-BF_4$)$_2EMI^+$.

Cellulose was then suspended in a solution of EMI$-BF_4$ and a new mass peak, potentially corresponding to (EMI$-BF_4$)($C_6H_{10}O_5$)$^+$, was detected in the resulting mass spectrum, with a respective mass-to-charge ratio of $m/z = 357.7$. These initial results show the ESI technique developed for space propulsion systems may be translatable to an ion source capable of preserving complex organic molecules for mass spectral analysis.

While arginine was not detected when suspended in EMI$-BF_4$, it may be possible to use EMI-Am as an alternative ionic liquid to measure this and other amino acid species. Future work will pursue methods of using EMI-Am as an effective solvent and ionic liquid for ESI-MS analysis of amino acids and other organics. Histidine monohydrochloride was successfully dissolved in EMI-Am, and future experiments will attempt to use a heater to decrease the resulting solution's viscosity such that it can be effectively employed as an ionic liquid with the current ESI-MS system.

Organics may also be dissolved into a water solution that is then in turn suspended in a solution of EMI$-BF_4$. This solution can then be placed into a vacuum chamber, where the residual water can be pumped out. This will leave a suspension of analyte molecules in the ionic liquid, even if they don't dissolve in it directly. If successful, not only will this be a useful laboratory technique for the study of hard-to-dissolve organics, but it will be more closely aligned with actual flight data from icy ocean worlds, where any potential biomolecules will presumably be entrained in water ice.

Histidine monohydrochloride readily dissolves in water, and it is an attractive amino acid for study due to the fact that it has never been observed in abiotic inventories and is thus only associated with biological systems [10]. Because of this and other reasons, histidine fragmentation in TOF-MS systems has been studied in a number of recent publications related to astrobiology surveys [17], [18], [19], including one from an author of the present study [20]. Future experiments with histidine will thus compare the performance of the ESI-MS system presented here with this literature, as well as more general chemistry studies of amino acids, e.g. [21]. This performance will also be compared between the potentially different operational regimes of the ESI-MS (i.e., water solutions pumped out of EMI$-BF_4$, direct dissolution into EMI-Am, other potential methods, etc.). Further studies may also

consider different ionic liquids, as these may be desirable for TOF-MS solutions either due to superior solvency of organics or due to relaxed instrument operation requirements.

Once baseline studies of histidine and other amino acids have been completed, higher mass organics and complex mixtures will be pursued. Solutions of several amino acids will be studied, as these are more biologically relevant than single amino acids [10], [22]. Following experiments will then consider a wide variety of biomolecules, to eventually include cellular material.

Finally, the small form factor of the prototype ESI-MS assemblies presented here allow for easy transport and integration into other experimental systems. While the present study uses a simple linear TOF-MS system, the source can be mounted to different mass spectrometer systems, potentially even at different scientific institutions. In this way, the performance of the ESI source can be studied in the context of higher performance mass spectrometer systems.

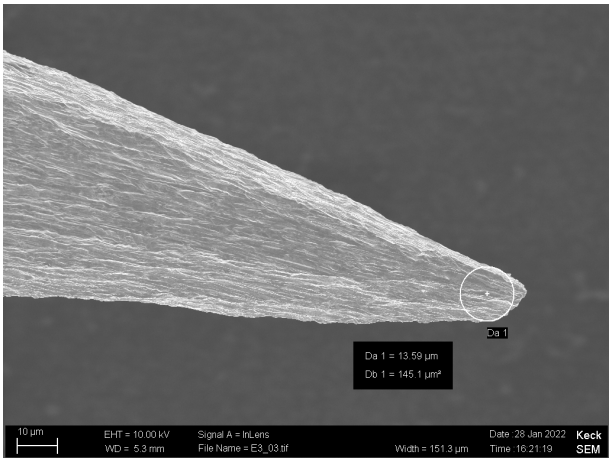

Figure 10. Tungsten needle sharpened to 13.6 μm and microetched.

ACKNOWLEDGMENT

This work made use of the Cornell Center for Materials Research Shared Facilities which are supported through the NSF MRSEC program (DMR-1719875).

A portion of the work was supported by an internal grant to AEH and EMP through the Jet Propulsion Laboratory, California Institute of Technology, under contract with the National Aeronautics and Space Administration (80NM0018D0004).

APPENDIX

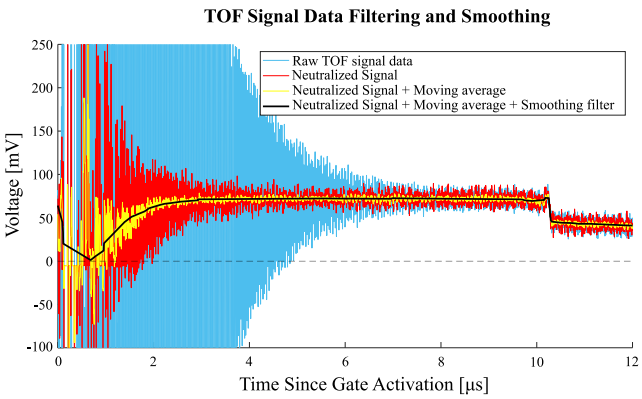

Figure 9. Filtering and smoothing of the TOF data including oscillations.

REFERENCES

[1] R. J. Cotter, "Time-of-flight mass spectrometry for the structural analysis of biological molecules," *Analytical Chemistry*, vol. 64, no. 21, pp. 1027A–1039A, 1992.

[2] F. Postberg, N. Khawaja, B. Abel, G. Choblet, C. R. Glein, M. S. Gudipati, B. L. Henderson, H.-W. Hsu, S. Kempf, F. Klenner *et al.*, "Macromolecular organic compounds from the depths of Enceladus," *Nature*, vol. 558, no. 7711, pp. 564–568, 2018.

[3] A. R. Hendrix, T. A. Hurford, L. M. Barge, M. T. Bland, J. S. Bowman, W. Brinckerhoff, B. J. Buratti, M. L. Cable, J. Castillo-Rogez, G. C. Collins *et al.*, "The NASA roadmap to ocean worlds," *Astrobiology*, vol. 19, no. 1, pp. 1–27, 2019.

[4] K. Reh, L. Spilker, J. I. Lunine, J. H. Waite, M. L. Cable, F. Postberg, and K. Clark, "Enceladus Life Finder: The search for life in a habitable moon," in *2016 IEEE Aerospace Conference*. IEEE, 2016, pp. 1–8.

[5] L. Chou, P. Mahaffy, M. Trainer, J. Eigenbrode, R. Arevalo, W. Brinckerhoff, S. Getty, N. Grefenstette, V. Da Poian, G. M. Fricke *et al.*, "Planetary mass spectrometry for agnostic life detection in the solar system," *Frontiers in Astronomy and Space Sciences*, p. 173, 2021.

[6] E. Petro, A. Bruno, P. Lozano, L. E. Perna, and D. Freeman, "Characterization of the TILE electrospray emitters," in *AIAA Propulsion and Energy 2020 Forum*, 2020, p. 3612.

[7] T. Roy, V. Hruby, N. Rosenblad, P. Rostler, and D. Spence, "Cubesat propulsion using electrospray thrusters," 2009.

[8] Y.-J. Kuan, S. B. Charnley, H.-C. Huang, W.-L. Tseng, and Z. Kisiel, "Interstellar glycine," *The Astrophysical Journal*, vol. 593, no. 2, p. 848, 2003.

[9] K. Altwegg, H. Balsiger, A. Bar-Nun, J.-J. Berthelier, A. Bieler, P. Bochsler, C. Briois, U. Calmonte, M. R. Combi, H. Cottin *et al.*, "Prebiotic chemicals—amino acid and phosphorus—in the coma of comet 67P/Churyumov-Gerasimenko," *Science advances*, vol. 2, no. 5, p. e1600285, 2016.

[10] P. G. Higgs and R. E. Pudritz, "A thermodynamic basis for prebiotic amino acid synthesis and the nature of the first genetic code," *Astrobiology*, vol. 9, no. 5, pp. 483–490, 2009.

[11] P. Lozano and M. Martinez-Sanchez, "Efficiency estimation of EMI-BF4 ionic liquid electrospray thrusters," in *41st AIAA/ASME/SAE/ASEE Joint Propulsion Conference & Exhibit*, 2005, p. 4388.

[12] C. Miller and P. C. Lozano, "Measurement of the fragmentation rates of solvated ions in ion electrospray

thrusters," in *52nd AIAA/SAE/ASEE Joint Propulsion Conference*, 2016, p. 4551.

[13] Z.-D. Ding, Z. Chi, W.-X. Gu, S.-M. Gu, J.-H. Liu, and H.-J. Wang, "Theoretical and experimental investigation on dissolution and regeneration of cellulose in ionic liquid," *Carbohydrate polymers*, vol. 89, no. 1, pp. 7–16, 2012.

[14] N. Takahashi, "Molecular dynamics modeling of ionic liquids in electrospray propulsion," Massachusetts Inst. of Tech, Cambridge, Tech. Rep., 2010.

[15] P. Lozano and M. Martínez-Sánchez, "Ionic liquid ion sources: characterization of externally wetted emitters," *Journal of Colloid and Interface Science*, vol. 282, no. 2, pp. 415–421, 2005.

[16] P. Lozano, B. Glass, and M. Martinez-Sanchez, "Performance characteristics of a linear ionic liquid electrospray thruster," in *29th International Electric Propulsion Conference*, vol. 9. Citeseer, 2005.

[17] J. A. Schulze, D. E. Yilmaz, M. L. Cable, M. Malaska, A. E. Hofmann, R. P. Hodyss, J. I. Lunine, A. C. van Duin, and A. Jaramillo-Botero, "Effect of salts on the formation and hypervelocity-induced fragmentation of icy clusters with embedded amino acids," *ACS Earth and Space Chemistry*, 2022.

[18] F. Klenner, F. Postberg, J. Hillier, N. Khawaja, M. L. Cable, B. Abel, S. Kempf, C. R. Glein, J. I. Lunine, R. Hodyss *et al.*, "Discriminating abiotic and biotic fingerprints of amino acids and fatty acids in ice grains relevant to ocean worlds," *Astrobiology*, vol. 20, no. 10, pp. 1168–1184, 2020.

[19] S. Burke, K. Hanold, R. Continetti, M. Miller, S. Waller, A. Jaramillo-Botero, R. Hodyss, M. Malaska, A. E. Hofmann, J. Lunine *et al.*, "Studies of molecular fragmentation of ice-entrained organics after hypervelocity impact," in *AGU Fall Meeting Abstracts*, vol. 2021, 2021, pp. A55L–1561.

[20] Z. Ulibarri, T. Munsat, M. Voss, J. Fontanese, M. Horányi, S. Kempf, and Z. Sternovsky, "Detection of the amino acid histidine and its breakup products in hypervelocity impact ice spectra," *Icarus*, vol. 391, p. 115319, 2023.

[21] P. Zhang, W. Chan, I. L. Ang, R. Wei, M. M. Lam, K. M. Lei, and T. C. Poon, "Revisiting fragmentation reactions of protonated α-amino acids by high-resolution electrospray ionization tandem mass spectrometry with collision-induced dissociation," *Scientific reports*, vol. 9, no. 1, pp. 1–10, 2019.

[22] M. L. Cable, M. Neveu, H.-W. Hsu, T. M. Hoehler, and R. Dotson, *Enceladus*. University of Arizona Press, 2020, pp. 217–246. [Online]. Available: http://www.jstor.org/stable/j.ctv105bb62.15

BIOGRAPHY

Shawn P. Cogan *is an M.Sc. student who completed his master's thesis at Cornell University. His research interests include spacecraft propulsion, space mission design, and numerical simulation. He is studying aerospace engineering at the University of Stuttgart, Germany, where he also received his bachelor's degree. During his studies, he interned at Airbus in the satellite mechanical design department, and was a member of the Stuttgart rocketry team.*

Zach Ulibarri *is a Postdoctoral Associate in the Advanced Space Transportation and Architecture (ASTRA) Lab at Cornell University. He received his Ph.D. in Physics from the University of Colorado. His research focuses on the use of time-of-flight mass spectrometry to study complex organics, such as amino acids or potential biomolecules, and isotopic ratios at icy ocean worlds.*

Elaine Petro *is an Assistant Professor of Mechanical and Aerospace Engineering at Cornell University where she directs the Advanced Space Transit and Architectures Laboratory. Her research interests include spacecraft electric propulsion, sustainable space exploration through in-situ resource utilization, and plasma science.*

Amy Hofmann *is a Research Scientist in the Planetary Science Section at NASA's Jet Propulsion Laboratory. She received her Ph.D. in Geochemistry from the California Institute of Technology. Her research focuses on elucidating the fundamental chemical physics that govern isotopic fractionation, as applied to various planetary systems, as well as the development of flight instrumentation to enable in situ interrogation of the same.*